

Low-Rank Discriminative Least Squares Regression for Image Classification

Zhe Chen, Xiao-Jun Wu*, and Josef Kittler, *Life Member, IEEE*

Abstract—Latest least squares regression (LSR) methods aim to learn slack regression targets to replace strict zero-one labels. However, the difference between intra-class targets can also be highlighted when enhancing the distance between different classes, and roughly pursuing relaxed targets may lead to the problem of overfitting. To solve above problems, we propose a low-rank discriminative least squares regression model (LRDLSR) for multi-class image classification. Specifically, LRDLSR class-wisely imposes low-rank constraint on the intra-class regression targets to encourage its compactness and similarity. Moreover, LRDLSR introduces an additional regularization term on the learned targets to avoid the problem of overfitting. We show that these two improvements help to learn a more discriminative projection for regression, thus achieving better classification performance. The experimental results over a range of image databases demonstrate the effectiveness of the proposed LRDLSR method.

Index Terms—least squares regression, low-rank regression targets, overfitting, image classification

I. INTRODUCTION

LEAST squares regression (LSR) is a very popular method in the field of multicategory image classification. LSR aims at learning a projection to transform the original data into the corresponding zero-one labels with a minimum loss. Over the past decades, many LSR based variants have been developed, such as locally weighted LSR [1], local LSR [2], LASSO regression [3], kernel ridge LSR [4], kernel LSR [5], weighted LSR [6], a least-squares support vector machine (LS-SVM) [7] and partial LSR [8]. Besides linear regression, sparse representation, collaborative representation, and probabilistic collaborative representation based classification methods (LRC, SRC, CRC and ProCRC) [9][10][11][12] also take advantage of the LSR framework to find representation coefficients.

However, there are still many issues associated with the above LSR based methods. First, taking the zero-one label matrix as the regression targets is too strict. It is not ideal for classification, as calculating the least squares loss between the extracted features and binary targets cannot reflect the classification performance of a regression model, especially in the multi-class conditions. For instance, the Euclidean distance of any two of the inter-class regression targets is

constant, i.e., $\sqrt{2}$, and for each sample, the difference between the targets of the true and the false class identically equals to 1. These characteristics are contrary to the expectation that the transformed inter-class features should be as far as possible from each other. To address this problem, some representative algorithms, i.e., discriminative LSR (DLSR) [13], retargeted LSR (ReLSR) [14], and groupwise ReLSR [15], were proposed to learn relaxed regression targets instead of the original binary targets. Concretely, DLSR utilizes the ε -dragging technique to encourage the inter-class regression targets moving in the opposite directions, thus enlarging the distances between different classes. Different from DLSR, ReLSR learns the regression targets from the original data rather than directly adopting the zero-one labels of the samples, in which the margins between classes are forced to be greater than 1. Lately, Wang et al. [14] proved that DLSR is a special model of ReLSR, with the translation values set to zero, and proposed a new formulation for ReLSR. With the new formulation, GReLSR introduces a groupwise constraint to guarantee that intra-class samples have similar translation values.

Besides, the traditional LSR based methods also do not take into account the data correlation during the projection learning procedure, which may result in the loss of some useful structural information and cause overfitting. To explore the underlying relationships, Fang *et al.* [16] constructed a class-compactness-graph to ensure that the projected intra-class features are compact so that the overfitting problem can be mitigated to some degree. Wen *et al.* [17] proposed a novel framework called inter-class sparsity based DLSR (ICS_DLSR), which introduces an inter-class sparsity constraint on the DLSR model to make the projected features of each class retain sparse structure. In fact, both, the RLRLR and ICS_DLSR algorithms, are based on the model of DLSR, that is they adopt the ε -dragging technique. In addition to learning slack regression targets, RLRL [19] proposed to jointly learn the latent feature subspace and classification model so that the data representation extracted is more discriminative and compact for classification. The learned latent subspace can be regarded as a transition between the original samples and binary labels.

The various measures adopted by the algorithms mentioned above improve the classification performance. However the ε -dragging technique or the margin constraint used to relax the label matrix also amplify the difference among the intra-class regression targets, which may deteriorate the classification performance. In this paper, a novel relaxed targets based regression model named low-rank discriminative least squares

*Corresponding author.

E-mail: wu_xiaojun@jiangnan.edu.cn

Zhe Chen and Xiao-Jun Wu are with the School of Internet of Things, Jiangnan University, Wuxi 214122, China.

Josef Kittler is with the Centre for Vision, Speech and Signal Processing (CVSSP), University of Surrey, Guildford GU2 7XH, U.K.

regression (LRDLSR) is proposed to learn a more discriminative projection. Based on the model of DLSR, LRDLSR classwise imposes a low-rank constraint on the relaxed regression targets to ensure the intra-class targets are compact and similar. In this way, the ε -dragging technique will be exploited to a better effect so that both the intra-class similarity and the inter-class separability of regression targets can be guaranteed. Moreover, LRDLSR minimizes the energy of the resulting dynamic regression targets to avoid the problem of overfitting.

The rest of this paper is organized as follows. First, the related works are briefly introduced in Section II. The proposed LRDLSR model and the corresponding optimization procedure are described in Section III. The properties of the algorithm are analysed in Section IV. The experimental results are presented in Section V and Section VI concludes this paper.

II. RELATED WORKS

In this section, we briefly review the related works. Let $X = [x_1, x_2, \dots, x_n] \in R^{d \times n}$ denote the n training samples from c classes ($c \geq 2$), where d is the dimensionality of the samples. $X_i \in R^{d \times n_i}$ denotes the subset of the samples belonging to the i th class. $H = [h_1, h_2, \dots, h_n] \in R^{c \times n}$ denote the binary label matrix of X , where column h_i of H , i.e., $h_i = [0, \dots, 0, 1, 0, \dots, 0]^T \in R^c$, corresponds to the training sample x_i . If sample x_i belongs to the p th class, then the p th element of h_i is 1 and all the others are 0.

A. Original LSR

The main idea of LSR is to learn a projection matrix that maps the original training samples into the binary label space. The objective function of LSR can be formulated as

$$\min_Q \|QX - H\|_F^2 + \lambda \|Q\|_F^2 \quad (1)$$

where $\|\bullet\|_F^2$ is the matrix Frobenius norm ($\|A\|_F^2 = \text{tr}(A^T A) = \text{tr}(A A^T)$) and λ is a positive regularization parameter. Q is the projection matrix. The first term in problem (1) is a least squares loss function, while the second term is used to avoid the problem of overfitting. Obviously, (1) has a closed-form solution as

$$\hat{Q} = HX^T (XX^T + \lambda I)^{-1} \quad (2)$$

Given a new sample y , LSR calculates its label as $k = \text{arg max}_j (Qy)_j$ where $(Qy)_j$ is the j th value of Qy .

B. DLSR and ReLSR

As previously said, making the regression features to pursue strict zero-one outputs is inappropriate for classification tasks. Unlike original LSR, DLSR [13] and ReLSR [14] aim at learning relaxed regression targets rather than using the binary labels H as their targets. The main idea of DLSR is to enlarge the distance between the true and the false classes by using an ε -dragging technique. Its regression model can be formulated as

$$\min_{Q, M} \|QX - (H + B \odot M)\|_F^2 + \lambda \|Q\|_F^2, \quad s.t. \quad M \geq 0 \quad (3)$$

where \odot denotes the Hadamard-product operator. $M \in R^{c \times n}$ is a non-negative ε -dragging label relaxation matrix. $B \in R^{c \times n}$ is a constant matrix which is defined as

$$B_{ij} = \begin{cases} +1, & \text{if } H_{ij} = 1 \\ -1, & \text{if } H_{ij} = 0 \end{cases} \quad (4)$$

Compared to the original LSR, it can be seen that the regression targets are extended to be $H' = H + B \odot M$ in DLSR. To help the understanding, we use four samples to explain why the new relaxed target matrix H' is more discriminative than H . Let x_1, x_2, x_3, x_4 be four training samples in which the first two samples are from the first class and the latter two are from the second class. Thus their binary label matrix is defined as

$$H = \begin{bmatrix} 1 & 1 & 0 & 0 \\ 0 & 0 & 1 & 1 \end{bmatrix} \in R^{2 \times 4} \quad (5)$$

It is obvious that the distance between any two inter-class targets is $\sqrt{2}$ ($\sqrt{(1-0)^2 + (0-1)^2} = \sqrt{2}$). Such a fixed distance cannot reflect the classification ability of regression model well. But if we use H' to replace H , then we have

$$H' = \begin{bmatrix} 1 + m_{11} & 1 + m_{12} & -m_{13} & -m_{14} \\ -m_{21} & -m_{22} & 1 + m_{23} & 1 + m_{24} \end{bmatrix} \quad (6)$$

In doing so, the distance between the first and the fourth target is $\sqrt{(1 + m_{11} + m_{14})^2 + (-m_{21} - 1 - m_{24})^2} \geq \sqrt{2}$ rather than a constant. The margin between the two classes is also enlarged by changing the regression outputs in the opposite directions. For example, the class margin of the first regression target is $1 + m_{11} + m_{21} > 1$. These meet the expectation that inter-class samples should be as far as possible from each other after being projected.

Likewise, ReLSR directly learns relaxed regression targets from the original data to ensure that samples are correctly classified with large margins. The ReLSR model is defined as

$$\begin{aligned} & \min_{Q, T, b} \|T - QX - be_n\|_F^2 + \lambda \|Q\|_F^2 \\ & s.t. T_{r_j, j} - \max_{i \neq r_j} T_{i, j} \geq 1, i = 1, 2, \dots, n \end{aligned} \quad (7)$$

where r_j indicates the true label of sample x_j . T is optimized from X with a large margin constraint which enhances the class separability. Hence ReLSR performs better flexibility than DLSR.

III. FROM DLSR AND ReLSR TO LRDLSR

A. Problem Formulation and New Regression Model

Although DLSR and ReLSR can learn soft targets and maintain the closed-form solution for the projection, an undue focus on large margins will also result in overfitting. As indicated before, exploiting the data correlations is helpful in learning a discriminative data representation. From the classification point of view, both, the intra-class similarity and the inter-class incoherence of regression targets should be promoted. However, DLSR and ReLSR ignore the former, because their relaxation values are dynamic. Hence the ε -dragging technique in DLSR and the margin constrain method in ReLSR will also promote the intra-class regression targets

to be discrete. If the intra-class similarity of learned targets is weakened, the discriminative power will be compromised. Therefore, based on the model of DLSR, we propose a low-rank discriminative least squares regression model (LRDLSR) as follows

$$\min_{Q,T,M} \frac{1}{2} \|QX - T\|_F^2 + \frac{\alpha}{2} \|T - (H + B \odot M)\|_F^2 + \beta \sum_{i=1}^c \|T_i\|_* + \frac{\gamma}{2} \|T\|_F^2 + \frac{\lambda}{2} \|Q\|_F^2, \text{ s.t. } M \geq 0 \quad (8)$$

where α, β, γ and λ are the regularization parameters and $\|\bullet\|_*$ denotes the nuclear norm (the sum of singular values). Q and T denote the projection matrix and the slack target matrix, respectively. The second term $\|T - (H + B \odot M)\|_F^2$ is used to learn relaxed regression targets with large inter-class margins, the third term $\sum_{i=1}^c \|T_i\|_*$ is used to learn similar intra-class regression targets, and the fourth term $\|T\|_F^2$ is used to avoid the overfitting problem of T .

With our formulation, we note that the major difference between our LRDLSR and DLSR is that in LRDLSR we encourage the relaxed regression targets of each class to be low-rank so that the compactness and similarity of the regression targets from each class can be enhanced. Combined with the ε -dragging technique, both the intra-class similarity and inter-class separability of regression targets will be preserved, thus producing a discriminative projection. In fact, the proposed class-wise low-rank constraint term can also be extended to the ReLSR and GReLSR models, or other relaxed target learning based LSR models. In addition to the above difference, we also add a simple F -norm constraint on T , i.e., $\|T\|_F^2$, to restrict the energy of the targets T . This is because there are no any restrictions on the variation magnitude of the dynamically updated regression targets in DLSR. In this way, the slack matrix, i.e., M , may be very fluctuant and discrete because of aggressively exploiting the largest class margins, thus leading to the problem of overfitting.

B. Optimization of LRDLSR

To directly solve the optimization problem in (8) is impossible because three variables Q, T and M are correlated. Therefore, an iterative update rule is devised to solve it so as to guarantee that it has a closed-form solution in each iteration. In this paper, the alternating direction multipliers method (ADMM) [20] is exploited to optimize LRDLSR. In order to make (8) separable, we first introduce an auxiliary variable P as follows

$$\min_{T,P,Q,M} \frac{1}{2} \|QX - T\|_F^2 + \frac{\alpha}{2} \|T - (H + B \odot M)\|_F^2 + \beta \sum_{i=1}^c \|P_i\|_* + \frac{\gamma}{2} \|T\|_F^2 + \frac{\lambda}{2} \|Q\|_F^2, \text{ s.t. } T = P, M \geq 0 \quad (9)$$

Then we obtain the augmented Lagrangian function of (9)

$$L(T, P, Q, M, Y) = \frac{1}{2} \|QX - T\|_F^2 + \frac{\alpha}{2} \|T - (H + B \odot M)\|_F^2 + \beta \sum_{i=1}^c \|P_i\|_* + \frac{\gamma}{2} \|T\|_F^2 +$$

$$\frac{\lambda}{2} \|Q\|_F^2 + \frac{\mu}{2} \|T - P + \frac{Y}{\mu}\|_F^2 \quad (10)$$

where Y is the Lagrangian multiplier, $\mu > 0$ is the penalty parameter. Next we update variables one by one.

Update T : By fixing variables P, Q, M , T can be obtained by minimizing the following problem

$$L(T) = \frac{1}{2} \|QX - T\|_F^2 + \frac{\alpha}{2} \|T - (H + B \odot M)\|_F^2 + \frac{\gamma}{2} \|T\|_F^2 + \frac{\mu}{2} \|T - P + \frac{Y}{\mu}\|_F^2 \quad (11)$$

Obviously, T has a closed-form solution as

$$T = (1 + \alpha + \gamma + \mu)^{-1} [QX + \alpha(H + B \odot M) + \mu P - Y] \quad (12)$$

Update P : Given T, Q and M , P can be class-wisely updated by

$$L(P_i) = \beta \|P_i\|_* + \frac{\mu}{2} \|T_i - P_i + \frac{Y_i}{\mu}\|_F^2 \quad (13)$$

We can use the singular value thresholding algorithm [21] to class-wisely optimize (13). The optimal solution of P_i is

$$P_i = I_{\frac{\beta}{\mu}}(T_i + \frac{Y_i}{\mu}) \quad (14)$$

where $I_{\zeta}(\Theta)$ is the singular value shrinkage operator.

(I) Given a matrix $\Theta \in R^{a \times b}$, its singular value decomposition can be formulated as

$$\Theta = U_{a \times r} \Sigma V_{b \times r}^T, \quad \Sigma = \text{diag}(\sigma_1, \dots, \sigma_r). \quad (15)$$

where r is the rank of Θ , U and V are column-orthogonal matrices.

(II) Given a threshold ζ ,

$$I_{\zeta}(\Theta) = U_{a \times r} \text{diag}(\{\max(0, \sigma_j - \zeta)\}_{1 \leq j \leq r}) V_{b \times r}^T. \quad (16)$$

Update Q : Analogously, Q can be solved by minimizing

$$L(Q) = \frac{1}{2} \|QX - T\|_F^2 + \frac{\lambda}{2} \|Q\|_F^2 \quad (17)$$

We set the derivative of $L(Q)$ with respect to Q to zero, and obtain the following closed-form solution

$$Q = TX^T (XX^T + \lambda I)^{-1} \quad (18)$$

Let $R = X^T (XX^T + \lambda I)^{-1}$, we find that R is independent of T , thus R can be pre-calculated before starting the iteration.

Update M : After optimizing T, P and Q , we can update the non-negative relaxation matrix M by

$$\min_M \|T - (H + B \odot M)\|_F^2, \text{ s.t. } M \geq 0 \quad (19)$$

Let $R = T - H$, according to [13], the optimal solution of M can be calculated by

$$M = \max(B \odot R, 0) \quad (20)$$

The optimization procedure of LRDLSR is overviewed in Algorithm 1.

Algorithm 1. Optimizing LRDLRSR by ADMM

Input: Normalized training samples X and its label matrix H ; Parameters $\alpha, \beta, \gamma, \lambda$.

Initialization: $T = P = H, Q = \mathbf{0}, M = \mathbf{1}^{c \times n}, Y = \mathbf{0}^{c \times n}, \mu_{max} = 10^8, tol = 10^{-6}, \mu = 10^{-5}, \rho = 1.1$.

While not converged do:

- 1) Update T by using Eq. (12).
- 2) Update P by using Eq. (13).
- 3) Update Q by using Eq. (18).
- 4) Update M by using Eq. (20).
- 5) Update Lagrange multipliers Y as

$$Y = Y + \mu(T - P). \quad (17)$$

- 6) Update penalty parameter μ as

$$\mu = \min(\mu_{max}, \rho\mu). \quad (18)$$

- 7) Check convergence:

$$if \|T - P\|_{\infty} \leq tol. \quad (19)$$

End While

Output: Q, T and M .

C. Classification

Once (8) is solved, we can obtain the optimal projection matrix Q . Then, we use Q to obtain the projection features of the training samples, i.e., QX . Suppose $y \in R^d$ is a test sample, then its projection feature is Qy . For convenience, we use the NN classifier to implement classification in our paper.

IV. ANALYSIS OF THE PROPOSED METHOD

A. Computational Complexity

In this section, we analyze the computational complexity of Algorithm 1. The main time-consuming steps of Algorithm 1 are

- (1) Singular value decomposition in Eq. (13).
- (2) Matrix inverse in (18).

Since the remaining steps only consist of simple matrix addition, subtraction and multiplication operations, and element-wise multiplication operation, similar to [17][18], we also ignore the time complexity of these operations. The complexity of singular value decomposition in Eq. (13) is $O(\min(cn_i^2, n_i c^2))$. The complexity of pre-computing $(XX^T + \lambda I)^{-1}$ in Eq. (14) is $O(d^3)$. Thus the final time complexity for Algorithm 1 is about $O(d^3 + \tau \sum_{i=1}^c \min[cn_i^2, c^2 n_i])$, where τ is the number of iterations.

B. Convergence validation

In this section, we experimentally validate the convergence property of the ADMM optimization algorithm. Fig. 1 gives an empirical evidence that Algorithm 1 converges very well. The value of objective function monotonically decreases with the increasing number of iterations in four different databases. This indicates the effectiveness of the optimization method. However, it is still arduous to theoretically demonstrate that our optimization algorithm has strong convergence because problem (8) has four different blocks and the overall model of LRDLRSR is non-convex.

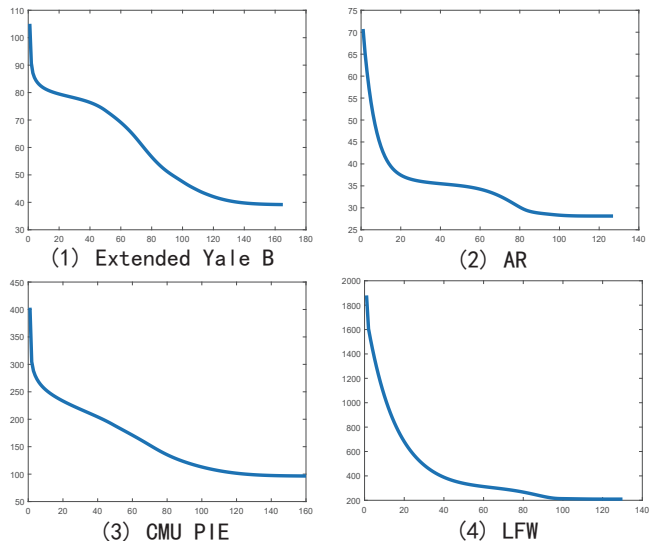


Fig. 1. Convergence curves and objective function versus iterations of LRDLRSR on four face datasets.

V. EXPERIMENTS

In order to verify the effectiveness of the proposed LRDLRSR model, we compare it with five state-of-the-art LSR model based classification methods, including DLSR [13], ReLSR [14], GReLSR [15], RLRLR[16] and RLSL[19], and three representation based classification methods, including LRC [9], CRC [11], ProCRC [12], on five real image datasets. For LRDLRSR, DLSR, ReLSR, GReLSR, RLRLR and RLSL, we use the NN classifier. For RLSL, the parameter d is set to $2c$, where c is the number of classes. When we test the performance of CRC, LRC and ProCRC, all the training samples are used as the dictionary. To make fair comparisons, we directly utilize the released codes of the methods being compared to conduct experiments and seek the best parameters for them as much as possible. All the experiments are repeated ten times with random splits of training and test samples. The average results and the standard deviations (mean±std) are reported. The image datasets used in our experiments can be divided into two types:

- (1) Face: the AR [22], the CMU PIE [23], the Extended Yale B [24] and the Labeled Faces in the Wild (LFW) [25] datasets;
- (2) Object: the COIL-20 [26] dataset.

A. Experiments for Object Classification

In this section, we validate the performance of our LRDLRSR model on the COIL-20 object dataset which has 1440 images of 20 classes. Each class consists of 72 images that are collected at pose intervals of 5 degrees. Some images from this database are shown in Fig. 2. In our experiments, all images are resized to 32×32 pixels. For each class, we randomly choose 10, 15, 20, 25 samples to train the model and treat all the remaining images as the test set. The average classification accuracies are reported in Table I. As shown in Table I, we find that our LRDLRSR algorithm achieves much better classification results than all the remaining methods used

TABLE I
RECOGNITION ACCURACY (MEAN± STD%) OF DIFFERENT METHODS ON THE COIL-20 OBJECT DATABASE.

Train No.	LRC	CRC	ProCRC	DLSR	ReLSR	GReLSR	RLRLR	RLSL	LRDLSR(ours)
10	92.30±1.15	89.09±1.48	90.61±0.95	93.27±1.43	93.65±1.94	90.98±1.62	92.61±1.04	94.80±1.16	95.12±1.22
15	94.89±1.33	92.58±1.27	94.53±0.85	96.25±0.75	96.75±0.72	93.60±0.83	94.86±0.85	96.09±0.90	97.78±0.86
20	97.49±0.51	94.15±1.15	96.17±0.82	97.52±0.67	98.17±0.67	95.65±0.82	96.27±0.33	97.45±0.29	98.51±0.85
25	98.32±0.60	94.99±1.24	97.53±0.68	98.67±0.53	98.90±0.85	96.30±0.84	96.76±1.06	97.66±0.91	99.24±0.59

TABLE II
RECOGNITION ACCURACY (MEAN± STD%) OF DIFFERENT METHODS ON THE EXTENDED YALE B FACE DATABASE.

Train No.	LRC	CRC	ProCRC	DLSR	ReLSR	GReLSR	RLRLR	RLSL	LRDLSR(ours)
10	82.18±0.92	91.85±0.61	91.74±0.86	87.95±1.10	89.68±0.94	88.46±1.00	90.21±0.84	89.02±0.88	91.18±0.65
15	89.43±0.58	94.76±0.66	95.41±0.76	93.37±0.99	93.98±0.52	93.13±0.82	94.80±0.64	93.29±0.73	95.07±0.66
20	92.00±0.77	96.39±0.56	96.74±0.26	95.73±0.68	96.14±0.54	95.25±0.50	96.37±0.71	95.18±0.62	96.84±0.36
25	93.73±0.79	97.69±0.40	97.58±0.37	97.34±0.55	97.75±0.64	97.06±0.37	97.34±0.50	96.69±0.63	98.16±0.46

TABLE III
RECOGNITION ACCURACY (MEAN± STD%) OF DIFFERENT METHODS ON THE AR FACE DATABASE.

Train No.	LRC	CRC	ProCRC	DLSR	ReLSR	GReLSR	RLRLR	RLSL	LRDLSR(ours)
3	28.73±0.99	71.42±0.59	76.16±1.12	73.58±1.63	73.53±1.47	74.77±1.45	76.39±1.56	75.70±1.01	78.80±0.76
4	37.21±1.13	78.50±0.67	83.58±0.82	80.47±1.36	81.46±0.79	82.54±1.24	83.55±1.35	83.02±0.79	86.20±0.45
5	44.69±1.22	83.54±0.67	87.33±0.74	85.33±0.93	86.43±0.94	87.35±1.21	86.68±0.54	86.37±0.40	90.16±0.75
6	52.95±1.54	86.79±0.71	90.32±0.66	88.18±0.78	88.98±0.99	89.96±0.73	89.41±0.89	88.80±0.48	92.23±0.80

TABLE IV
RECOGNITION ACCURACY (MEAN± STD%) OF DIFFERENT METHODS ON THE CMU PIE FACE DATABASE.

Train No.	LRC	CRC	ProCRC	DLSR	ReLSR	GReLSR	RLRLR	RLSL	LRDLSR(ours)
10	75.67±1.01	86.39±0.60	89.00±0.37	87.54±0.79	88.18±0.79	86.88±0.72	91.15±0.58	87.70±0.63	91.57±0.48
15	85.26±0.63	91.14±0.43	92.18±0.25	92.22±0.54	92.29±0.42	91.21±0.51	93.52±0.32	91.38±0.43	94.45±0.51
20	89.84±0.48	93.08±0.35	93.94±0.18	94.12±0.27	94.23±0.21	93.39±0.27	94.78±0.30	93.03±0.38	95.83±0.35
25	92.55±0.39	94.12±0.30	94.58±0.21	95.25±0.20	95.53±0.16	94.32±0.31	95.40±0.18	94.04±0.27	96.59±0.21

in the comparison, which proves the effectiveness of LRDLSR for the object classification tasks.



Fig. 2. Some images from the COIL-20 object database.

B. Experiments for Face Classification

In this section, we evaluate the classification performance of LRDLSR on four real face datasets.

(1) The *Extended Yale B Dataset*: The Extended Yale B database consists of 2414 face images of 38 individuals. Each individual has about 59-64 images. All images are resized to 32×32 pixels in advance. We randomly select 10, 15, 20, and 25 images of each individual as training samples, and set the remaining images as test samples.

(2) The *AR Dataset*: We select a subset which consists of 2600 images of 50 women and 50 men and use the projected

540-dimensional features provided in [27]. In each individual, we randomly select 3, 4, 5, and 6 images as training samples and the remaining images are set as test samples.

(3) The *CMU PIE Dataset*: We select a subset of this dataset where each individual has 170 images that are collected under five different poses (C05, C07, C09, C27 and C29). All images are resized to 32×32 pixels. We randomly select 10, 15, 20, and 25 images of each individual as training samples, and treat the remaining images as test samples.

(4) The *LFW Dataset*: Similar to [17], we use a subset of this dataset which consists of 1251 images of 86 individuals to conduct experiments. Each individual has 11-20 images. In our experiments, all images are resized to 32×32 . We randomly select 5, 6, 7, and 8 images from each individual as training samples and use the remaining images to test. Some images from the above four face databases are shown in Fig. 3.

The average classification rates on these four face datasets are reported in Tables II-V, respectively. It can be observed that our LRDLSR outperforms all the other algorithms on the four face datasets. The main reason is that our LRDLSR can simultaneously guarantee the intra-class compactness and the inter-class irrelevance of slack regression targets so that more

TABLE V
RECOGNITION ACCURACY (MEAN \pm STD%) OF DIFFERENT METHODS ON THE LFW FACE DATABASE.

Train No.	LRC	CRC	ProCRC	DLSR	ReLSR	GReLSR	RLRLR	RLSL	LRDLSR(ours)
5	29.99 \pm 2.21	31.67 \pm 1.16	33.19 \pm 0.99	30.43 \pm 1.38	31.43 \pm 1.13	36.76 \pm 1.37	36.21 \pm 1.60	36.10 \pm 1.82	37.20\pm1.66
6	32.37 \pm 1.36	34.27 \pm 1.04	35.90 \pm 0.93	32.35 \pm 1.62	34.46 \pm 1.51	39.22 \pm 0.92	39.37 \pm 1.65	38.48 \pm 1.59	39.99\pm1.22
7	35.53 \pm 1.69	35.96 \pm 1.40	36.87 \pm 1.55	34.67 \pm 2.45	37.50 \pm 2.61	43.02 \pm 2.19	42.03 \pm 1.42	41.43 \pm 1.58	43.82\pm1.23
8	36.98 \pm 1.82	37.92 \pm 1.50	38.24 \pm 1.15	36.27 \pm 1.65	38.72 \pm 1.22	44.39 \pm 1.77	43.30 \pm 1.59	42.18 \pm 1.37	44.88\pm1.58

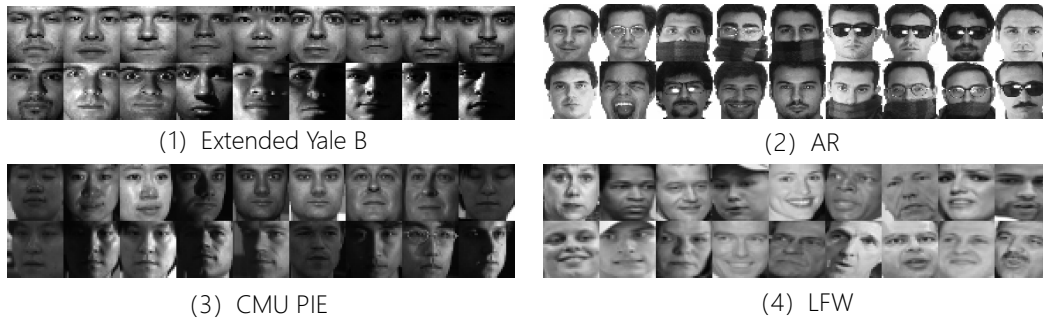


Fig. 3. Some images from face datasets.

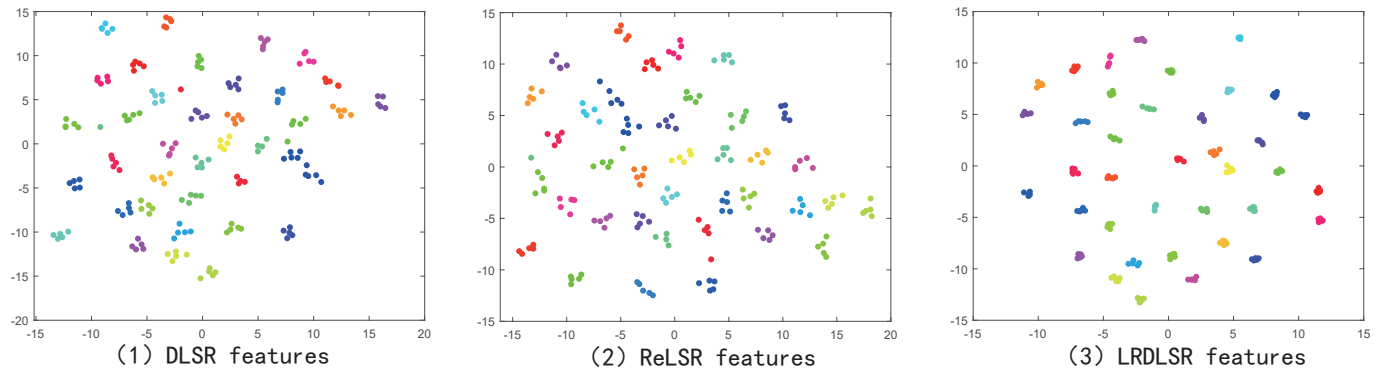


Fig. 4. T-SNE visualization results of the features extracted by different algorithms on the Extended Yale B database.

TABLE VI
RECOGNITION ACCURACIES (MEAN \pm STD%) OF LRDLRSR AND LRDLRSR WITHOUT LOW-RANK CONSTRAINT.

Database	AR (6)	EYB (15)	CMU PIE (15)	LFW (8)	COIL-20 (15)
LRDLRSR	92.21\pm0.54	94.67\pm0.87	94.64\pm0.28	45.56\pm0.63	97.78\pm0.85
LRDLRSR($\beta = 0$)	86.77 \pm 1.25	93.39 \pm 0.53	90.56 \pm 0.32	36.50 \pm 1.60	94.48 \pm 0.99

discriminative information is preserved during the projection learning. It is worth noting that the standard deviation of accuracies of LRDLRSR are also competitive which demonstrates the robustness of LRDLRSR. Besides, we find that the performance gain of LRDLRSR is significant when the number of training samples per subject is small, which indicates our model is applicable to small-sample-size problems. Fig. 4 shows the t-SNE [28] visualization of the features on the Extended Yale B dataset which are extracted by DLSR, ReLSR and LRDLRSR, respectively. We randomly select 5 samples for each individual to validate. It is obvious that the features extracted by LRDLRSR model present ideal inter-class separability and intra-class compactness which is favorable to

classification.

In order to verify whether the low-rank constraint is useful, we set the parameter $\lambda = 0$, then test its classification performance. We randomly select 6, 15, 15, 8, and 15 samples per class as the training samples, from the AR, Extended Yale B, CMU PIE, LFW and COIL-20 database, and the remaining samples are treated as test samples. We repeat all experiments ten times and report the average results. The comparative results are shown in Table VI. It is apparent that for $\beta = 0$, the classification performance is degraded. Especially on the LFW database, the difference is actually more than 9%, which indicates that pursuing low-rank intra-class regression targets is indeed helpful to classification.

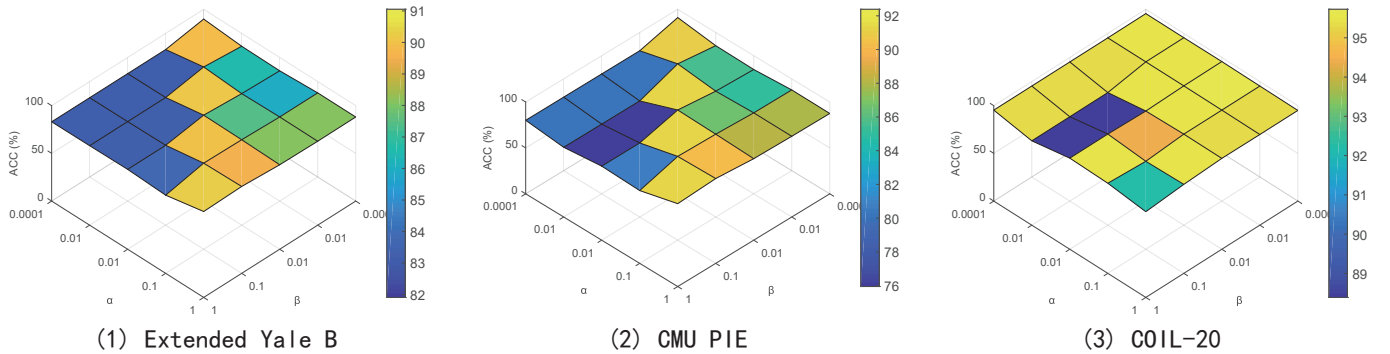


Fig. 5. The performance evaluation (%) of LRDLRSR versus parameters α and β on three different datasets where randomly selected 10 samples for each class are used to train our model.

C. Classification using deep features

In this section, we conduct experiments on the COIL-20, CMU PIE and LFW databases to further verify whether our model is also effective for deep features. In our experiments, two deep networks, VGG16 [29] and ResNet50 [30], are used. After obtaining the deep features of the original samples, since the dimensionality of features is very high, we first conduct a dimensionality reduction by using PCA so that 98% of the energy of features is preserved. For the CMU PIE and COIL-20 databases, we randomly select 10 samples of each class for training and all the remaining samples are used for testing. For the LFW database, we randomly select 5 samples of each class for training. Similarly, we repeat all the experiments ten times and report the mean accuracy and standard deviation (mean \pm std) of the different algorithms. The experimental results are shown in Table VII. We see that both VGG and ResNet features can achieve better classification accuracy than the original features. Especially on the LFW database, there is nearly a 20% improvement. Our LRDLRSR model with deep features is consistently superior to other algorithms which means that LRDLRSR is also appropriate for the deep features.

D. Parameter Sensitivity Validation

Up to now, it is still an unresolved problem to select optimal parameters for different datasets. In this section, we conduct a sensitivity analysis of the parameters of our LRDLRSR model. Note that there are four parameters, i.e., α , β , γ and λ to be selected in LRDLRSR. Among them, α and β are respectively used to balance the weight of the slack targets learning term and the class-wise low-rank targets learning term, γ and λ are respectively used to avoid the overfitting problem of learned targets T and the projection matrix Q . For convenience, we set the parameters γ and λ to 0.01 in advance and focus on selecting the optimal values of parameters α and β from the candidate set $\{0.0001, 0.001, 0.01, 0.1, 1\}$ by cross-validation. The classification accuracy as a function of different parameter values on three datasets is shown in Fig. 5. It is apparent that the optimal parameters are different on the respective datasets, but our LRDLRSR model is not very sensitive to the values of α and β . This also demonstrates that compact and similar intra-class targets are critical to discriminative projection learning,

TABLE VII
CLASSIFICATION ACCURACIES (MEAN \pm STD%) ON THE DEEP FEATURES OF THE COIL-20, CMU PIE AND LFW DATABASES.

Database	COIL-20 (10)	CMU PIE (10)	LFW (5)
LRDLRSR (ours)	95.12 \pm 1.22	91.57 \pm 0.48	37.20 \pm 1.66
VGG+LRDLRSR (ours)	98.65\pm1.09	91.74 \pm 0.47	55.48 \pm 1.55
ResNet+LRDLRSR (ours)	98.59 \pm 0.63	92.98\pm0.54	56.19\pm1.06
RLSL	94.80 \pm 1.16	87.70 \pm 0.63	36.10 \pm 1.82
VGG+RLSL	97.44 \pm 0.72	89.05 \pm 0.46	53.89 \pm 2.12
ResNet+RLSL	97.61\pm1.31	89.69\pm0.48	54.10\pm1.22
RLRLR	92.61 \pm 1.04	91.15 \pm 0.58	36.21 \pm 1.60
VGG+RLRLR	98.60\pm0.58	91.55 \pm 0.45	55.15 \pm 1.47
ResNet+RLRLR	98.40 \pm 0.67	93.66\pm0.40	55.43\pm1.55
GReLSR	90.98 \pm 1.62	86.88 \pm 0.72	36.76 \pm 1.37
VGG+GReLSR	97.79\pm0.86	87.04 \pm 0.63	52.18 \pm 1.57
ResNet+GReLSR	97.73 \pm 0.67	89.87\pm0.37	52.85\pm1.53
ReLSR	93.65 \pm 1.94	88.18 \pm 0.79	31.43 \pm 1.13
VGG+ReLSR	96.90 \pm 1.06	88.77 \pm 0.41	51.88 \pm 1.42
ResNet+ReLSR	96.92\pm0.89	89.84\pm0.53	52.91\pm1.75
DLSR	93.27 \pm 1.43	87.54 \pm 0.79	30.43 \pm 1.38
VGG+DLSR	96.84\pm1.43	87.47 \pm 0.82	49.84 \pm 1.95
ResNet+DLSR	96.70 \pm 1.65	89.66\pm0.63	52.07\pm1.91

but the classification performance does not completely depend on the choice of the parameters.

VI. CONCLUSION

In this paper, we proposed a low-rank discriminative least squares regression (LRDLRSR) model for multi-class image classification. LRDLRSR aims at improving the intra-class similarity of the regression targets learned by the ε -dragging technique. This can ensure that the learned targets are not only relaxed but also discriminative, thus leading to more effective projection. Besides, LRDLRSR introduces an extra regularization term to avoid the problem of overfitting by restricting the energy of learned regression targets. The experimental results on the object and face databases demonstrate the effectiveness of the proposed method.

ACKNOWLEDGMENT

This work is supported by the National Natural Science Foundation of China under Grant Nos. 61672265, U1836218,

the 111 Project of Ministry of Education of China under Grant No. B12018, and UK EPSRC Grant EP/N007743/1, MURI/EPSRC/DSTL GRANT EP/R018456/1.

REFERENCES

- [1] D. Ruppert and M. P. Wand, "Multivariate locally weighted least squares regression," *Ann. Statist.*, vol. 22, no. 33, pp. 13461370, 1994.
- [2] Ruppert, D., Sheather, S. J., & Wand, M. P, "An effective bandwidth selector for local least squares regression," *J. Amer. Statist. Assoc.*, 90(432), 12571270, 1995.
- [3] R. Tibshirani, "Regression shrinkage and selection via the lasso," *J. Roy. Statist. Soc. B (Methodol.)*, vol. 58, no. 1, pp. 267-288, 1996.
- [4] S. An, W. Liu, and S. Venkatesh, "Face recognition using kernel ridge regression," in *Proc. IEEE Comput. Soc. Conf. Comput. Vis. Pattern Recognit.*, Minneapolis, MN, USA, pp. 1-8, Jun. 2007.
- [5] Gao, J., Shi, D., & Liu, X. , "Significant vector learning to construct sparse kernel regression models," *Neural Netw.*, 20(7), 791-798, 2007.
- [6] T. Strutz, "Data Fitting and Uncertainty: A Practical Introduction to Weighted Least Squares and Beyond," Wiesbaden, Germany: Vieweg, 2010.
- [7] L. Jiao, L. Bo, and L. Wang, "Fast sparse approximation for least squares support vector machine," *IEEE Trans. Neural Netw.*, vol. 18, no. 3, pp. 685-697, May 2007.
- [8] Abdi, H., "Partial least squares regression and projection on latent structure regression (pls regression)", *Wiley Interdiscip. Rev. Comput. Stat.*, 2(1), 97-106, 2010.
- [9] I. Naseem, R. Togneri, and M. Bennamoun, "Linear regression for face recognition," *IEEE Trans. Pattern Anal. Mach. Intell.*, vol. 32, no. 11, pp. 2106-2112, 2010.
- [10] J. Wright, A.Y. Yang, A. Ganesh, et al, "Robust face recognition via sparse representation," *IEEE Trans. Pattern Anal. Mach. Intell.*, vol. 31, no. 2, pp. 210-227, 2009.
- [11] L. Zhang, M. Yang, and X. Feng, "Sparse representation or collaborative representation: Which helps face recognition?" in *Proc. of IEEE Int. Conf. Comput. Vis.*, pp. 471-478, 2011.
- [12] S. Cai, L. Zhang, W. Zuo, et al, "A probabilistic collaborative representation based approach for pattern classification," in *Proc. of IEEE Conf. Comput. Vis. Pattern Recognit.*, pp. 2950-2959, 2016.
- [13] S. M. Xiang, F. P. Nie, G. F. Meng, C. H. Pan, and C. S. Zhang, "Discriminative least squares regressions for multiclass classification and feature selection," *IEEE Trans. Neural Netw. Learn. Syst.*, vol. 23, no. 11, pp. 1738-1754, Nov. 2012.
- [14] X.-Y. Zhang, L. Wang, S. Xiang, and C.-L. Liu, "Retargeted least squares regression algorithm," *IEEE Trans. Neural Netw. Learn. Syst.*, vol. 26, no. 9, pp. 2206-2213, Sep. 2015.
- [15] L. Wang and C. Pan, "Groupwise retargeted least-squares regression," *IEEE Trans. Neural Netw. Learn. Syst.*, vol. 29, no. 4, pp. 1352-1358, Apr. 2018.
- [16] X. Fang, Y. Xu, X. Li, Z. Lai, W. K. Wong, and B. Fan, "Regularized label relaxation linear regression," *IEEE Trans. Neural Netw. Learn. Syst.*, vol. 29, no. 4, pp. 1006-1018, Apr. 2018.
- [17] J. Wen, Y. Xu, Z. Y. Li, Z. L. Ma, Y. R. Xu, "Inter-class sparsity based discriminative least square regression," *Neural Networks*, 102: 36-47, 2018.
- [18] Z. Chen, X. J. Wu, J. Kittler, "A sparse regularized nuclear norm based matrix regression for face recognition with contiguous occlusion". *Pattern Recognition Letters*, 2019.
- [19] X. Z. Fang, S. H. Teng, Z. H. Lai, et al. "Robust latent subspace learning for image classification," *IEEE transactions on neural networks and learning systems*, 29(6): 2502-2515, 2018.
- [20] E. Chu B. Peleato S. Boyd, N. Parikh and J. Eckstein, "Distributed optimization and statistical learning via the alternating direction method of multipliers," *Found. Trends Mach. Learn.*, pages 1-122, 2011.
- [21] J. F. Cai, E. J. Candes, and Z. Shen, A singular value thresholding algorithm for matrix completion, *SIAM J. Optimization*, vol. 20, no. 4, pp. 1956-1982, 2010.
- [22] A. M. Martinez and R. Benavente, "The AR face database," *CVC*, New Delhi, India, Tech. Rep. 24, 1998.
- [23] T. Sim, S. Baker, M. Bsat, The CMU pose, illumination, and expression (PIE) database, in *Proc. of IEEE Int. Conf. Autom. Face Gesture Recognit.*, pp. 46-51, 2002.
- [24] A. S. Georghiadis, P. N. Belhumeur, and D. Kriegman, From few to many: Illumination cone models for face recognition under variable lighting and pose, *IEEE Trans. Pattern Anal. Mach. Intell.*, vol. 23, no. 6, pp. 643-660, Jun. 2001.
- [25] G. B. Huang, M. Ramesh, T. Berg, and E. Learned-Miller, Labeled faces in the wild: A database for studying face recognition in unconstrained environments, *College Comput. Sci.*, Univ. Massachusetts, Amherst, MA, USA, Tech. Rep. 07-49, Oct. 2007.
- [26] S. A. Nene, S. K. Nayar and H. Murase, Columbia Object Image Library (COIL-100), Technical Report, CUCS-006-96, 1996.
- [27] L.S. Davis Z. Jiang, Z. Lin. "Label consistent k-svd: Learning a discriminative dictionary for recognition," *IEEE Transactions on Pattern Analysis and Machine Intelligence*, pages 2651-2664, 2013.
- [28] Y. LeCun Y.-L. Boureau, F. Bach and J. Ponce. Learning mid-level features for recognition. in *Proc. 23rd IEEE Conf. Comput. Vis. Pattern Recognit.*, pages 2559-2566, 2010.
- [29] K. Simonyan, A. Zisserman. "Very deep convolutional networks for large-scale image recognition." *arXiv preprint arXiv:1409.1556*, 2014.
- [30] K. He, X. Zhang, S. Ren, et al. "Deep residual learning for image recognition"//*Proceedings of the IEEE conference on computer vision and pattern recognition*. 2016: 770-778.